DEPARTMENT OF INFORMATICS

TECHNISCHE UNIVERSITÄT MÜNCHEN

Master's Thesis in Quantum Computing

Quantum and Classical Generative Modeling for Quantum States Preparation

Wiktor Jurasz

DEPARTMENT OF INFORMATICS

TECHNISCHE UNIVERSITÄT MÜNCHEN

Master's Thesis in Quantum Computing

Quantum and Classical Generative Modeling for Quantum States Preparation

Quantenbasierte und klassische generative Modellierung zur Erzeugung von Quantenzuständen

Author:	Wiktor Jurasz
Supervisor:	Prof. Dr. Christian Mendl
Submission Date:	15.07.2021

I confirm that this master's thesis in quantum computing is my own work and I have documented all sources and material used.

Munich, 15.07.2021   Wiktor Jurasz

Acknowledgments

Abstract

Kurzfassung

Contents

1. Introduction

1.1. Problem Statement

Generative Modeling aims to learn a conditional probability $P(X|Z = z)$, where X is some observable variable and Z is a target variable. With knowledge of this conditional probability, it is possible to generate new observations $\bar{x} \in X$. In general case, one would not try to obtain the probability $P(X|Z)$ exactly, but learn an approximation. To do so a set of samples $x \in X$ is necessary to train a generator function $G : Z \to X$ which given a target variable $z \in Z$ generates new observation $x \in X$.

In the generative framework, the variable X is a multidimensional vector, in particular it can be used to describe an arbitrary quantum state. With this setup, given a finite set of quantum states $\mathcal{Q} = \{|\psi_i\rangle\}, |\psi_i\rangle \in X \forall i$ the generator function G prepares a new quantum state $|\hat{\psi}\rangle$. This new quantum state is expected to come from the same distribution as the samples in the input set $\mathcal{Q}$.

The only missing piece in the above description is the target variable Z. In the context of the function G, generating the quantum states, we can think about Z as a label of the generated state. That is, for a specific $z \in Z$ the function G always generates the same $|\hat{\psi}\rangle$.

In this work we evaluate different approaches to find the probability $P(X|Z = z)$ by learning the function G. We also address the limitations of the existing methods propose a new one that combines quantum and classical generative modeling.

1.2. Previous Work

There exist many different types of generative models. In this work we focus on one particular type, namely Generative Adversarial Networks (GANs). First version of GANs was proposed bu Goodfellow et al. [1] (to which we refer as Standard GANs - SGANs), since then many different variations of GANs were invented [2][3][4]. In context of this work, particularly interesting are Wasserstein GANs (WGANs)[5] which minimize *Earth-Mover* distance between two probability distribution (see Chapter 3) instead of *Jensen–Shannon* divergence (see Chapter 3) as in SGANs.

In recent years there has been an increasing interest in realizing Generative Adversarial Networks in Quantum Computing (QC) realm. Dallaire-Demers et al. proposed QuGANs [6] - Quantum Generative Adversarial Networks where generator and discriminator are parametrized quantum circuits. Similarly Benedetti et al. proposed fully quantum GANs for pure state approximation [7], but with different (more suitable for

NISQ [8]) learning method. Hybrid methods were also explored, Zoufal et al. build qGAN [9] - with parametrized quantum circuit as the generator and classical neural network as the discriminator.

De Palma et al. proposed quantum equivalent of Wasserstein distance of order 1 [10] which made the Quantum Wasserstein GANs (QWGANs) [11] possible. This variation of quantum GANs consist of the parametrized quantum circuit as the generator and the classical linear program as the discriminator.

1.3. Our Contribution

There has been a substantial effort in the direction of bringing GANs into the quantum realm. Nevertheless, this is still very early stage and many more routs are yet to be explored. In this work we focus on building quantum GANs that can generate new, unseen before, quantum states. Majority of models proposed so far are only able to generate the states the has been a part of the training data. Only some architectures [6] account for random noise in the input that allows to generate unseen states. However, as we discuss later, those are mostly theoretical and do not seem to work well in practice.

We propose a new quantum-classical hybrid approach that allows to generate an unlimited number of unseen quantum states. We utilize the fully quantum and fully classical generative models that work together in one framework.

We proceed as follows. In Chapter 2 we introduce briefly the quantum computing concepts necessary to understand the problems we are solving. We also establish the quantum computing notation used in the reminder of this work. In Chapter 3 we give a general introduction to classical GANs. In Chapter 4 we combine the knowledge from the previous chapters to introduce the concept of quantum GANs and talk more about the different variations of quantum GANs and their limitations. In Chapter 5 we introduce and describe in depth about our concept of hybrid quantum-classical generative framework. In Chapter **??** we and analyse numerous experiments with the proposed framework. We empirically prove the quality of the states generated by the proposed framework. Finally, in Chapter 6 we conclude our finding and talk briefly about the possible future directions.

2. Quantum Computing Introduction

In this chapter we provide a very brief introduction to the key concepts of quantum computing and introduce the notation used in the rest of this paper.

2.1. Parametric Circuits

3. Generative Adversarial Networks Introduction

Generative Adversarial Network (GAN)[1] is a machine learning framework designed to estimate generative models using adversarial process. At the core it consists of two models: the generative one G which is capable of learning the distribution of the provided data and discriminative model D that, given a data point, estimates whether it comes from input data or was generated by G. The models are set to compete with each other in a minmax game. D is trained to maximize the probability of correctly distinguishing between the generated and real samples, while G is trained to minimize it.

To approximate the true distribution p_r over data X we define a prior noise distribution p_z over noise input Z and the generator distribution p_g over data X. The generator represents a mapping $G(z \sim Z; \theta_g) \to x \sim X$, where θ_g is some learnable parameter (summary in Table 3.1).

The discriminator $D(x, \theta_d) \to [0; 1]$ is a function that given a sample $x \sim X$ outputs the probability whether x comes from data or was generated by G.

In classical GANs both G and D are most often modeled as multi-layer perceptrons[1] or other types of neural networks (e.g. convolutional neural networks [4]). However, there exist many different variations of cost functions used during the mixmax training procedure. In the following paragraphs we take a closer look at two of them, namely SGANs and WGANs, which are the most relevant in the context of this work. To simply the notation, we skip the θ parameters, i.e. $G(z, \theta_g) = G(z)$ and $D(x, \theta_d) = D(x)$

3.1. Standard Generative Adversarial Networks (SGANs)

The goal of D is to distinguish between the real and generated samples. For $x \sim X$ the output $D(x)$ should approach 1, while for $x \sim G(z)$ it should approach 0. In other terms it simultaneously maximizes $\mathbb{E}_{x \sim p_r(x)}[\log D(x)]$, and $\mathbb{E}_{z \sim p_z(z)}[\log 1 - D(G(z))]$.

Probability Distribution	Description
p_z	True distribution over noise input Z
p_g	Approximated distribution over input data X given by G
p_r	True distribution over input data X

Table 3.1.: Description of the probability distributions used in GANs

Generator G has an opposite objective, thus it minimizes the $\mathbb{E}_{z \sim p_z(z)}[\log 1 - D(G(z))]$. Putting it all together, we get the objective for SGANs 3.1.

$$
\begin{aligned}
\min_G \max_D \mathcal{L}(\mathcal{G}, \mathcal{D}) &= \min_G \max_D \mathbb{E}_{x \sim p_r(x)}[\log D(x)] + \mathbb{E}_{z \sim p_z(z)}[\log 1 - D(G(z))] \\
&= \min_G \max_D \mathbb{E}_{x \sim p_r(x)}[\log D(x)] + \mathbb{E}_{x \sim p_g(x)}[\log 1 - D(x)]
\end{aligned}
\tag{3.1}
$$

It can be shown, that if D is optimal, this loss function measures the similarity between p_r and p_g according to Jensen–Shannon divergence (see Appendix A.1 for detailed analysis).

SGANs are a very powerful tool, however, the training process is very difficult and unstable [12]. Additionally, if the data exists in low dimensional manifold (which seems to be the case for most real world data [13]), p_r and p_g are very likely disjoint and we are always capable of finding the perfect discriminator [14]. This might seem like a good characteristic, but if we examine the loss function closer, we find that it makes generator incapable of learning. For the perfect D we have $\forall x \sim X, D(x) = 1$ and $\forall z \sim Z, D(G(z)) = 0$. For those values $\mathcal{L}(\mathcal{G}, \mathcal{D}) = 0$ gradient vanishes and the gradient based optimizers cannot improve the generator anymore.

3.2. Wasserstein Generative Adversarial Networks (WGANs)

One of the very prominent improvement to SGANs and a way to mitigate the vanishing gradient problem is changing the cost function to use Wasserstein Distance.

The Wasserstein Distance, also called Earth-Mover's Distance is a distance measure between two probability distributions. The name "Earth Mover" comes from the fact, that informally the distance can be described as follows: Given two probability distributions, if we imagine them as piles of dirt, the "Earth Mover" distance says what is the minimum cost of turning one pile of dirt into the other one. Where cost is the volume that has to be moved times the distance is has to be moved.

The main advantage of the Wasserstein Distance over Jensen–Shannon Divergence is, that even in the case of disjoint distribution we get meaningful, stable distance which is well suited for gradient based learning.

Formally, the Wasserstein or Earth-Mover's Distance (EM Distance) is defined as follows:

$$
W(p_r, p_g) = \inf_{\gamma \in \Pi(p_r, p_g)} \mathbb{E}_{(x,y) \sim \gamma}[\|x - y\|]
\tag{3.2}
$$

Where $\Pi(p_r, p_g)$ denotes the set of all possible joint distributions, $\gamma(x, y)$ says how much "dirt" has to be transported in order to transform p_g into p_r. Since we take inf, the EM Distance is then the cost of such transport done in the optimal way.

The computation in 3.2 is highly intractable, but according to Kantorovich-Rubinstein duality [15], we can rewrite it as follows.

$$W(p_r, p_g) = \frac{1}{K} \sup_{\|f\|_L < K} \mathbb{E}_{x \sim p_r}[f(x)] - \mathbb{E}_{x \sim p_g}[f(x)] \qquad (3.3)$$

Where the supremum is overall all K-Lipschitz functions f. In practice it is impossible to go over all such functions. Instead we define a family of parameterized functions $\{f_w\}_{w \in W}$ and using the same notation for the generator as in SGANs the WGANs objective becomes

$$\max_f \min_G \mathcal{L}(f, G) = \max_f \min_G \mathbb{E}_{x \sim p_r}[f_w(x)] - \mathbb{E}_{z \sim p_z}[f_w(G_\theta(z))] \qquad (3.4)$$

.

Here the function f_w represents the "discriminator", however it does not anymore tries to distinguish between real and fake samples. Instead it is trained to to approximate K-continous Lipschitz function and compute the Wasserstein distance. The one missing part from the Equation 3.4 is ensuring the f_w Lipschitz continuity, this can be achieved by gradient clipping [5] or gradient penalty [16].

4. Quantum Generative Adversarial Networks

The field of Quantum Machine Learning (QML) is still in very early stages and there has been an ongoing effort on translating the classical Machine Learning (ML) concepts into QML realm. Because of the limitations of current quantum computers (NISQ) [17] and overall different paradigm of Quantum Computing (QC), this process is difficult and there is no clear answer to the question "how this concept should be realized on QC device?". While in classical GANs generator and discriminator are realized as deep neural networks, NISQ devices are not yet powerful enough to support such architecture. Instead parametric quantum circuits [18] are used.

In this chapter we take a closer look at two different designs of quantum GANs. We briefly explain theory behind them and show the results of our evaluation. The quantum GANs introduced in this chapter are the base of our hybrid classical-quantum generative framework.

4.1. Standard Quantum GANs (SQGANs)

In the classical GANs, both the discriminator and generator are deep, general purpose neural networks. The logical extension of this design in the quantum realm is to model those are general purpose parametric quantum circuits. This idea was formalized by Dallaire-Demers et al. [6] in the architecture we call SQGANs (Figure 4.1). The generator starts in the state $|0\rangle^{\otimes n}$ in the **Our R/G** wire, where n is the dimension of the real quantum samples. Additionally, the generator takes the label state $|\lambda\rangle$ in the **Label R/G** wire and the random state $|z\rangle$ that provides the entropy in the **Batch R/G** wire. The label state $|\lambda\rangle$ lets the generator to learn the conditional distribution $p_g(x|\lambda)$ instead of $p_g(x)$, this design was inspired by classical Conditional GANs [2]. The discriminator takes the generated state ρ_λ^G or real state ρ_λ^R and the corresponding label $|\lambda\rangle$ in the **Label D** wire, it also uses the workspace **Batch D** initialized in $|0\rangle$ state. The measurement on the single qubit wire **Out D** corresponds to the probability of the state in **Out R/G** being real or generated.

There are not any particular restrains on how G and D circuits should look like. However, to be able to learn and differentiate between arbitrary quantum states the ansatz used should be universal (i.e. be able to generate every quantum state given appropriate depth). The ansatz used in this work is described in details in Appendix A.2.
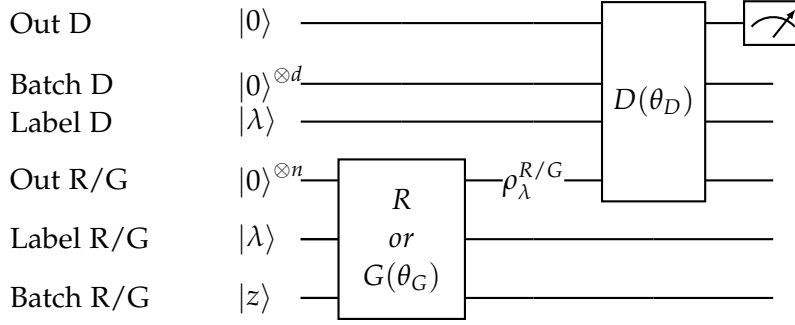
Figure 4.1.: SQGANs schema. The discriminator *D* and the generator *G* are parametric quantum circuits. The first 3 wires go directly to the discriminator. **Out D** outputs the probability of the input being generated. **Batch D** is an additional workspace of the discriminator and **Label D** contains the label state. **Out R/G** carries the generated or real state. **Label R/G** contains the label state and **Batch R/G** is the noise source for the generator, not used with the real samples.

4.1.1. Training

As in the SGANs we are interested in the minmax game setting. Specifically, in the **Out D** wire, the measurement of $|1\rangle$ indicates that the sample was real and $|0\rangle$ that the state was generated by *G*. [1] This should be the case for each label state $|\lambda\rangle$, which gives the objective 4.1.

$$
\max_D \min_G \mathcal{L}(G, D) =
$$

$$
\max_D \min_G \frac{1}{\Lambda} \sum_{\lambda \in \Lambda} P((D(\theta_D, |\lambda\rangle, R(\lambda)) = |1\rangle) \wedge (D(\theta_D, |\lambda\rangle, G(\theta_G, |\lambda\rangle, |z\rangle) = |0\rangle))))
$$
(4.1)

Where the discriminator objective is to maximize the probability of measuring $|1\rangle$ given real sample and measuring $|0\rangle$ given generated state. At the same time for the generator the objective is to do the opposite.

The SQGANs cost function 4.1 in contrast to the SGANs cost function 3.1 is not defined with log-likelihood. In quantum setup is more natural to work with linear functions and since the log is convex, the optimum is the same for both.

The cost function $\mathcal{L}(G, D)$ expressed in terms of measurements and assuming equal probability of sampling from *R* and *G* takes the form 4.1

$$
\mathcal{L}(G, D) = \frac{1}{2} + \frac{1}{4\Lambda} \sum_{\lambda \in \Lambda} tr((\rho_\lambda^{DR}(\theta_D) - \rho_\lambda^{DG}(\theta_D, \theta_G, z))Z)
$$
(4.2)

For detailed derivation on how to get from 4.1 to 4.1 refer to Appendix A.4.

---

[1] Using $|1\rangle$ and $|0\rangle$ in this order is just a convention we assume. Any other orthogonal pair can be used.

Gradient Estimation

To optimize the parameters θ_D and θ_G classical gradient descent method was used. First, the value of the cost function $\mathcal{L}(G, D)$ was estimated by sampling from the circuit 4.1. This allows to calculate the gradient w.r.t. θ_D and θ_G on classical computer and update the parameters at the step k in the following way

$$\theta_D^{k+1} = \theta_D^k + \alpha_D^k \nabla_{\theta_D} \mathcal{L}(\theta_G^k, \theta_D^k)$$
$$\theta_G^{k+1} = \theta_G^k - \alpha_G^k \nabla_{\theta_G} \mathcal{L}(\theta_G^k, \theta_D^k)$$

(4.3)

where α_D^k and α_G^k are learning rate metaparameters that can depend on the step k.

It is also possible to estimate the gradient directly on quantum computer by creating an explicit quantum circuit for each element of vectors θ_D/θ_G and reading the grading by sampling for those circuits [6].

4.1.2. Evaluation Results

Experimental Setup

In all of the experiments the real samples are generated by evaluating the circuit from Figure 4.2. This circuit was constructed by Smith et al. [19] to study topological phase transitions. All the gates in the circuit are parameterized by a single real valued parameter $g \in [-1; 1]$. The detailed gates layout is described in Appendix A.3.
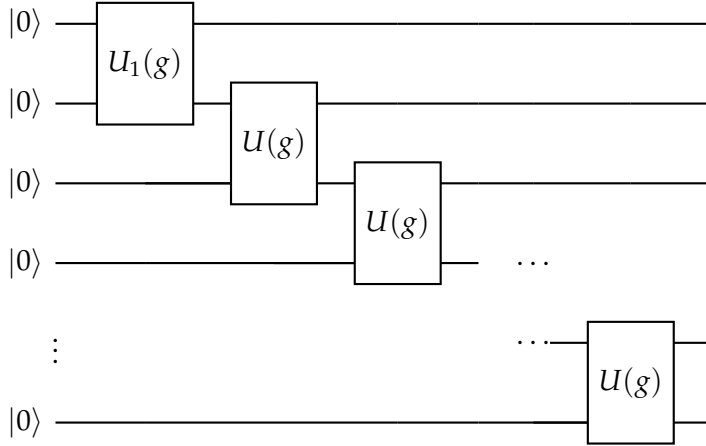

Figure 4.2.: The circuit used for generating real samples. All the gates are parametrized by a real valued parameter $g \in [-1; 1]$. For detailed description of the circuit see Appendix A.3

The generator and discriminator are both build using the generic circuit architecture from Appendix A.2. The number of layers differs and is specified for each experiment separately.

In all the experiment we use Adam optimizer [**kingma2017adam**] with parameters $\beta_1 = 0.9$, $\beta_2 = 0.98$, $\hat{\epsilon} = 1e - 9$. The learning rate is calculated as

$$lr = \max\left(\exp\left(-\frac{(k + 200) * \ln 100}{4000}\right), 0.01\right) \quad (4.4)$$

where k is the optimization step number. The learning rate decreases from ~ 0.8 to 0.01 in the first 3800 steps and then remains at 0.01 for the rest of the training. The exact values were derived experimentally and show overall good convergence. The exact number of epochs and iterations is specified for each experiment separately.

Results For Pure State Real Input

In this setup the generator is fed the same real input state at every iteration. The real input state is generated using circuit from Figure 4.2 for random $g \in [-1; 1]$.

In Figure 4.3 we present the results of experiments for different widths of the real input circuit. For All the experiments, the generator and discriminator were built using ansatz from Appendix A.2 for each layer. The **Label** and **Batch** wires are not used for any circuit.

For each real input width the generator was able to approximate the real source, increasing the fidelity as the training progressed. The training was harder for the bigger real source circuits and it can be clearly seen that the results for wider inputs are worse. Not only the final fidelity is lower, but also it fluctuates much more. It is also much harder for the generator to fool the discriminator for wider inputs.

It is not surprising that it is more difficult to train circuits with more qubits. We also acknowledge that with different metaparameters or optimization method the results could be better. However, our best results for more than 5 qubits in the real source are not longer useful for the real source approximation.

Results For Mixed State Real Input

If the real input source can provide more than one state, we can say that the generator is learning mixed state of all the input states. Dallaire-Demers et al. [6] trained a simple 2 qubits circuit with two real input states $|0\rangle$ or $|1\rangle$. In this setup **Label** wires consist of one qubit and also takes values $|0\rangle$ or $|1\rangle$, effectively learning $CNOT$ gate. This strategy do not have generalize well in to more complex cases. First, if there is more than one non-$|0\rangle$ input state, there would have to be a separate $CNOT$ gate for each state. Second, the number of qubits necessary for the **Label** wires grows logarithmically with the number of real input states. Both of those cause the circuit to grow in width and depth.

Another approach we explored was to insert $R_x(\lambda_k)$ parametrized rotation gates between each layer of the generator and discriminator. The generator is essentially learning how to rotate input state $|0\rangle$ to some desired real input state $|r_k\rangle$. Then, if for each k the rotation is pushed in different direction, the final generator might give different output state for each λ_k. However, in our experiments the generator was always

Fidelity between real and generated state

Probability of classifying generated state as real
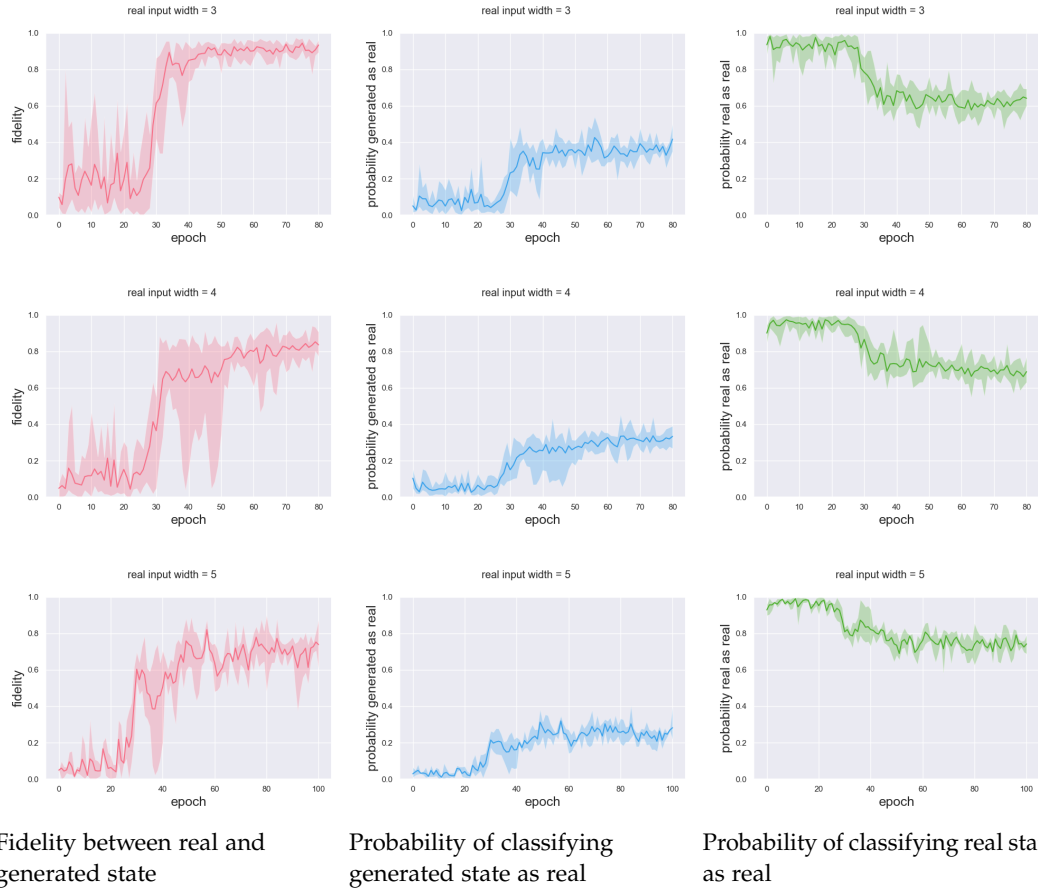
Probability of classifying real state as real

Figure 4.3.: The solid line represents the average value and the shaded area represents the range from 5 different experiments. The generator has the number of layers equal to the width of real input the discriminator has one more layer than the generator. In each epoch generator is optimized for 11 iterations and discriminator for 111.

learning to ignore the $R_x(\lambda_k)$ and in the end was only able to produce one, slightly distorted, state independent of λ_k.

4.1.3. Conclusions

4.2. Wasserstein Quantum GANs (WQGANs)

Theoretical description and experimental results

5. Unknown Quantum State Generation

5.1. Labeled State Generation

5.2. Unlabeled State Generation

6. Conclusions

A. Appendix

A.1. SGANs approximate Jensen–Shannon Divergence

A.2. SQGANs Ansatz

A.3. Topological Phase Transition Ansatz

A.4. SQGANs Cost Function

A.5. Optimizer Setup

Short description of Adam and meta parameters used (they change in different setting, so it must be mentioned in the main text)

B. Figures

List of Figures

List of Tables

Bibliography

[1] I. J. Goodfellow, J. Pouget-Abadie, M. Mirza, B. Xu, D. Warde-Farley, S. Ozair, A. Courville, and Y. Bengio. *Generative Adversarial Networks*. 2014. arXiv: 1406.2661 [stat.ML].

[2] M. Mirza and S. Osindero. *Conditional Generative Adversarial Nets*. 2014. arXiv: 1411.1784 [cs.LG].

[3] T. Karras, S. Laine, and T. Aila. *A Style-Based Generator Architecture for Generative Adversarial Networks*. 2019. arXiv: 1812.04948 [cs.NE].

[4] A. Radford, L. Metz, and S. Chintala. *Unsupervised Representation Learning with Deep Convolutional Generative Adversarial Networks*. 2016. arXiv: 1511.06434 [cs.LG].

[5] M. Arjovsky, S. Chintala, and L. Bottou. *Wasserstein GAN*. 2017. arXiv: 1701.07875 [stat.ML].

[6] P.-L. Dallaire-Demers and N. Killoran. "Quantum generative adversarial networks". In: *Physical Review A* 98.1 (July 2018). ISSN: 2469-9934. DOI: 10.1103/physreva.98.012324. URL: http://dx.doi.org/10.1103/PhysRevA.98.012324.

[7] M. Benedetti, E. Grant, L. Wossnig, and S. Severini. "Adversarial quantum circuit learning for pure state approximation". In: *New Journal of Physics* 21.4 (Apr. 2019), p. 043023. ISSN: 1367-2630. DOI: 10.1088/1367-2630/ab14b5. URL: http://dx.doi.org/10.1088/1367-2630/ab14b5.

[8] J. Preskill. "Quantum Computing in the NISQ era and beyond". In: *Quantum* 2 (Aug. 2018), p. 79. ISSN: 2521-327X. DOI: 10.22331/q-2018-08-06-79. URL: http://dx.doi.org/10.22331/q-2018-08-06-79.

[9] C. Zoufal, A. Lucchi, and S. Woerner. "Quantum Generative Adversarial Networks for learning and loading random distributions". In: *npj Quantum Information* 5.1 (Nov. 2019). ISSN: 2056-6387. DOI: 10.1038/s41534-019-0223-2. URL: http://dx.doi.org/10.1038/s41534-019-0223-2.

[10] G. D. Palma, M. Marvian, D. Trevisan, and S. Lloyd. *The quantum Wasserstein distance of order 1*. 2020. arXiv: 2009.04469 [quant-ph].

[11] B. T. Kiani, G. D. Palma, M. Marvian, Z.-W. Liu, and S. Lloyd. *Quantum Earth Mover's Distance: A New Approach to Learning Quantum Data*. 2021. arXiv: 2101.03037 [quant-ph].

[12] T. Salimans, I. Goodfellow, W. Zaremba, V. Cheung, A. Radford, and X. Chen. *Improved Techniques for Training GANs*. 2016. arXiv: 1606.03498 [cs.LG].

[13]   H. Narayanan and S. Mitter. "Sample Complexity of Testing the Manifold Hypothesis". In: *Proceedings of the 23rd International Conference on Neural Information Processing Systems - Volume 2*. NIPS'10. Vancouver, British Columbia, Canada: Curran Associates Inc., 2010, pp. 1786–1794.

[14]   M. Arjovsky and L. Bottou. *Towards Principled Methods for Training Generative Adversarial Networks*. 2017. arXiv: 1701.04862 [stat.ML].

[15]   C. Villani. "Optimal transport – Old and new". In: vol. 338. Jan. 2008, pp. xxii+973. DOI: 10.1007/978-3-540-71050-9.

[16]   I. Gulrajani, F. Ahmed, M. Arjovsky, V. Dumoulin, and A. Courville. *Improved Training of Wasserstein GANs*. 2017. arXiv: 1704.00028 [cs.LG].

[17]   K. Bharti, A. Cervera-Lierta, T. H. Kyaw, T. Haug, S. Alperin-Lea, A. Anand, M. Degroote, H. Heimonen, J. S. Kottmann, T. Menke, W.-K. Mok, S. Sim, L.-C. Kwek, and A. Aspuru-Guzik. *Noisy intermediate-scale quantum (NISQ) algorithms*. 2021. arXiv: 2101.08448 [quant-ph].

[18]   M. Schuld, A. Bocharov, K. M. Svore, and N. Wiebe. "Circuit-centric quantum classifiers". In: *Physical Review A* 101.3 (Mar. 2020). ISSN: 2469-9934. DOI: 10.1103/physreva.101.032308. URL: http://dx.doi.org/10.1103/PhysRevA.101.032308.

[19]   A. Smith, B. Jobst, A. G. Green, and F. Pollmann. *Crossing a topological phase transition with a quantum computer*. 2020. arXiv: 1910.05351 [cond-mat.str-el].